



## Regional Neural Activation Defines a Gateway for Autoreactive T Cells to Cross the Blood-Brain Barrier

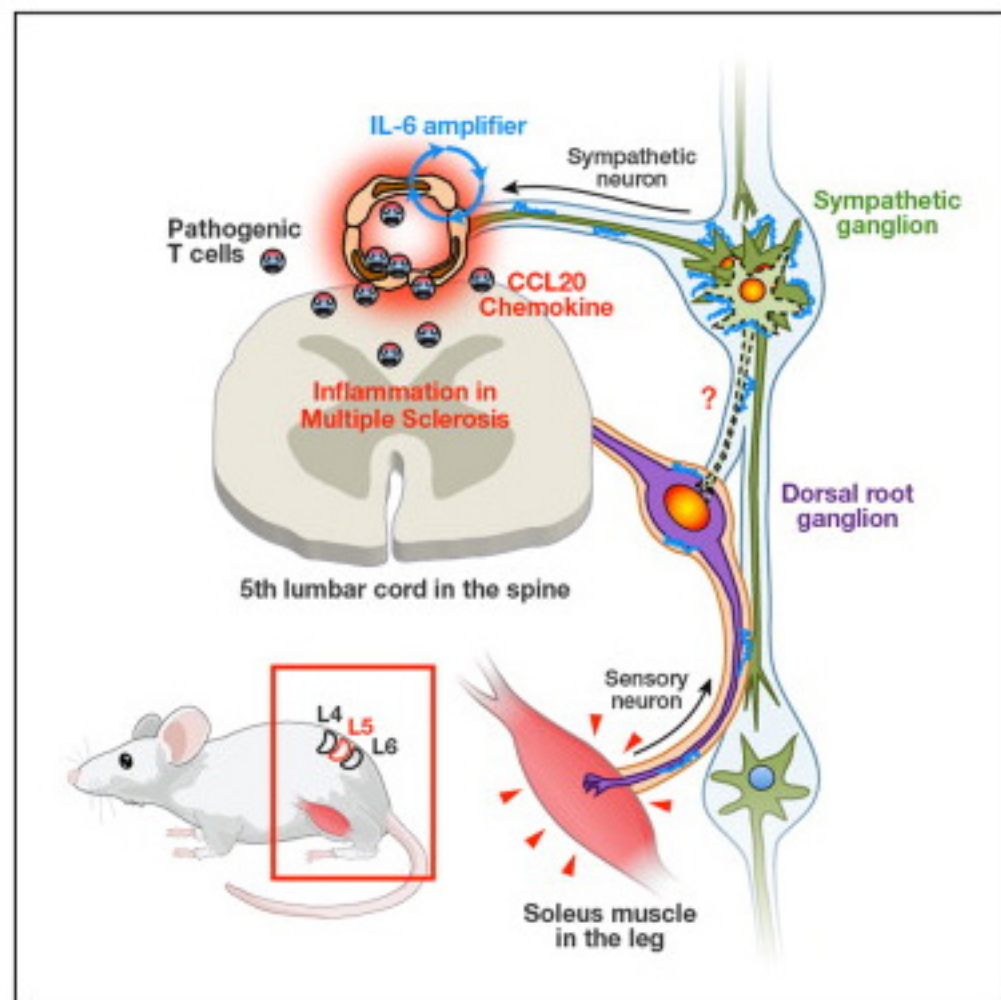
Original Research Article

Pages 447-457

Yasunobu Arima, Masaya Harada, Daisuke Kamimura, Jin-Haeng Park, Fuminori Kawano, Fiona E. Yull, Tadafumi Kawamoto, Yoichiro Iwakura, Ulrich A.K. Betz, Gabriel Márquez, Timothy S. Blackwell, Yoshinobu Ohira, Toshio Hirano, Masaaki Murakami

[Show preview](#) | [PDF \(1015 K\)](#) | [Supplementary content](#) | [Related articles](#) | [Related reference work articles](#)

### Graphical Abstract



# Regional Neural Activation Defines a Gateway for Autoreactive T Cells to Cross the Blood-Brain Barrier

Yasunobu Arima,<sup>1</sup> Masaya Harada,<sup>1</sup> Daisuke Kamimura,<sup>1</sup> Jin-Haeng Park,<sup>1</sup> Fuminori Kawano,<sup>2</sup> Fiona E. Yull,<sup>3</sup> Tadafumi Kawamoto,<sup>5</sup> Yoichiro Iwakura,<sup>6</sup> Ulrich A.K. Betz,<sup>7</sup> Gabriel Márquez,<sup>8,10</sup> Timothy S. Blackwell,<sup>3,4</sup> Yoshinobu Ohira,<sup>2</sup> Toshio Hirano,<sup>1,9</sup> and Masaaki Murakami<sup>1,\*</sup>

<sup>1</sup>Laboratory of Developmental Immunology, JST-CREST, Graduate School of Frontier Biosciences, Graduate School of Medicine, and WPI Immunology Frontier Research Center, Osaka University, Osaka 565-0871, Japan

<sup>2</sup>Department of Health and Sports Sciences, Graduate School of Medicine, and Graduate School of Frontier Biosciences, Osaka University, Osaka 560-0043, Japan

<sup>3</sup>Department of Cancer Biology

<sup>4</sup>Department of Medicine

Vanderbilt University, TN 37232, USA

<sup>5</sup>Radioisotope Research Institute, Department of Dental Medicine, Tsurumi University, Yokohama 230-8501, Japan

<sup>6</sup>Center for Experimental Medicine and Systems Biology, Institute of Medical Science, The University of Tokyo, Tokyo 108-8639, Japan

<sup>7</sup>Merck KGaA, Portfolio Development Merck Serono, 64293 Darmstadt, Germany

<sup>8</sup>National Center for Biotechnology (CNB-CSIC), Darwin 3, 28049 Madrid, Spain

<sup>9</sup>Laboratory of Cytokine Signaling, RIKEN Research Center for Allergy and Immunology, Yokohama 230-0045, Japan

<sup>10</sup>Present address: Genetrix SL, Plaza de la Encina, 10–11 Tres Cantos, 28760 Madrid, Spain

\*Correspondence: murakami@molonc.med.osaka-u.ac.jp

DOI 10.1016/j.cell.2012.01.022

## SUMMARY

Although it is believed that neural activation can affect immune responses, very little is known about the neuroimmune interactions involved, especially the regulators of immune traffic across the blood-brain barrier which occurs in neuroimmune diseases such as multiple sclerosis (MS). Using a mouse model of MS, experimental autoimmune encephalomyelitis, we show that autoreactive T cells access the central nervous system via the fifth lumbar spinal cord. This location is defined by IL-6 amplifier-dependent upregulation of the chemokine CCL20 in associated dorsal blood vessels, which in turn depends on gravity-induced activation of sensory neurons by the soleus muscle in the leg. Impairing soleus muscle contraction by tail suspension is sufficient to reduce localized chemokine expression and block entry of pathogenic T cells at the fifth lumbar cord, suggesting that regional neuroimmune interactions may offer therapeutic targets for a variety of neurological diseases.

## INTRODUCTION

Neuroimmune interactions arise from at least two types of pathways (Felten, 2000; Sternberg, 2006; Thayer and Sternberg, 2010; Watkins and Maier, 1999): neurohormonal pathways that depend on circulating hormones such as cortisol and catechol-

amines including norepinephrine, and neural pathways that are mainly mediated by direct neural connections with lymphoid organs like the thymus, bone marrow, spleen, and lymph nodes. Detailed anatomical analysis has suggested the lymphoid organs are innervated by the peripheral nervous system (Sternberg, 2006), the sympathetic nervous system (Nance and Sanders, 2007), and the parasympathetic nervous system (Tracey, 2007). Thus, neurohormonal pathways likely regulate immune responses systemically, while neural pathways regulate immune responses at a local and regional level, resulting in regional property differences even within the same organ. Although the systemic effects of neurohormonal pathways have been well investigated, little is known about the mechanisms used by the local neural pathways.

The central nervous system (CNS) is an immune-privileged environment, protected by the blood-brain barrier, which is formed by specific vessels tightly attached to each other (Galea et al., 2007; Wilson et al., 2010). This barrier, however, can be compromised upon the invasion of certain pathogens and/or latent infections (McGavern and Kang, 2011; Salinas et al., 2010), suggesting that immune cells in the peripheral lymphoid organs contribute to CNS related immune responses. However, how these cells enter and/or accumulate in the CNS from peripheral lymphoid organs is unclear. Moreover, although pathogenic CD4<sup>+</sup> T cells, which express high levels of cytokines such as IL-17A and IFN $\gamma$  and include autoreactive cells in peripheral lymphoid organs, are believed to play an essential role in the pathogenesis of MHC class II-associated autoimmune diseases like multiple sclerosis (MS) (Reboldi et al., 2009; Wilson et al., 2010), the initial gates of entry through the blood-brain barrier have yet to be analyzed, particularly at the molecular level. It is

known that leukocytes like CD4<sup>+</sup> T cells migrate into the CNS through the choroid plexus and subarachnoid space, brain regions that show excess chemokine levels, including the CCL20 chemokine, specifically in late phases of disease development, suggesting that pathogenic CD4<sup>+</sup> T cells can migrate from the blood directly into the brain tissues during these phases (Ransohoff, 2009; Reboldi et al., 2009; Wilson et al., 2010). Further, it has been hypothesized that barrier properties and/or the vasculature itself differ between CNS compartments and that these differences may influence immune cell access (Wilson et al., 2010). We hypothesize that these differences may arise from regional neural activation around the vessels, such that regional neural activation can regulate immune cell/blood cell accumulation in the CNS.

An important mediator for this regulation may be the NF $\kappa$ B-triggered positive-feedback-loop for IL-6 expression (IL-6 amplifier) in endothelial cells, which line blood and lymphatic vessels. We previously showed that this feedback loop is a synergistic activator of NF $\kappa$ B and STAT3 in type 1 collagen<sup>+</sup> cells after IL-17A and IL-6 stimulation. Activation of the IL-6 amplifier can lead to excess expression of various chemokines and cytokines including CCL20 and IL-6 and the development of autoimmune diseases like F759 arthritis and experimental autoimmune encephalomyelitis (EAE), which is a multiple sclerosis model induced by a myelin oligodendrocyte glycoprotein (MOG)-derived autopeptide immunization (Hirano, 2010; Murakami et al., 2011; Ogura et al., 2008). Additionally, those reports found that IL-6 amplifier activation in mouse joints directly or indirectly causes accumulation of various immune cell/blood cell populations including IL-17A- and IFN $\gamma$ -expressing pathogenic CD4<sup>+</sup> T cells there. Knowing this, we examined whether endothelial cell stimulation that depends on neural activity can trigger the IL-6 amplifier to cause regional pathogenic CD4<sup>+</sup> T cell migration into the CNS. We demonstrate that regional neural activation defines a gateway for autoreactive T cells to cross the blood-brain barrier via the IL-6 amplifier activation in endothelial cells at the fifth lumbar cord.

## RESULTS

### Transfused Pathogenic CD4<sup>+</sup> T Cells Mainly Migrate to the CNS via the Fifth Lumbar Cord during the Early Stages of Autoimmune Disease Development

To discover the gates of entry into the CNS for immune cells including pathogenic CD4<sup>+</sup> T cells, we employed a passive transfer method for EAE induction as described previously (Ogura et al., 2008). Pathogenic CD4<sup>+</sup> T cells were isolated from wild-type C57BL/6 mice immunized with a MOG peptide plus adjuvants (see the *Experimental Procedures*) and then cultured *in vitro* with bone marrow-derived dendritic cells in the presence of the same MOG peptide plus IL-23. The resulting pathogenic CD4<sup>+</sup> T cells contained Th1 and Th17 cells and were intravenously transferred into wild-type C57BL/6 mice. EAE development peaked at about 10–12 days after the transfer (Figure S1A available online).

It has been reported pathogenic CD4<sup>+</sup> T cells accumulate in the choroid plexus from day 13 after EAE induction by systemic immunizations in C57BL/6 mice (Reboldi et al., 2009). We found

no T cell accumulation around the choroid plexus during the first 5 days after pathogenic CD4<sup>+</sup> T cell transfer in untreated mice (data not shown). Because we have observed that pathogenic T cells mainly accumulate in the spinal cord around day 10 of EAE development (Sawa et al., 2009), we hypothesized that pathogenic CD4<sup>+</sup> T cells do not directly migrate to the choroid plexus, but may accumulate in the spinal cord instead, making the spinal cord a candidate for the gate in our model. We therefore investigated CD4<sup>+</sup> T cell numbers in the spinal cord over first 5 days. We first investigated pathogenic CD4<sup>+</sup> T cell accumulation in the CNS by using anterior-posterior whole mount sections after the transfer, finding robust pathogenic CD4<sup>+</sup> T cell accumulation in the lumbar level, but not in the thoracic and cervical levels of the spinal cord (data not shown). We then analyzed the lumbar level in detail. Because more than 95% of accumulated mononuclear cells merged with a congenic marker having pathogenic CD4<sup>+</sup> T cells, we measured pathogenic CD4<sup>+</sup> T cells by counting mononuclear cell numbers in five different spinal sections (see Figure 1A legend), took the average and then calculated the relative number of pathogenic CD4<sup>+</sup> T cells, finding a significant accumulation of pathogenic CD4<sup>+</sup> T cells in the fifth lumbar cord (Figure 1A), a result confirmed by flow cytometry (Figure 1B). The accumulation was much greater in the dorsal blood vessels of the fifth spinal cord than in the ventral ones (Figure 1C), suggesting dorsal blood vessels of the fifth spinal cord may be the gate to the CNS.

### Activation of the IL-6 Amplifier Plays a Role in the Accumulation of Pathogenic CD4<sup>+</sup> T Cells in the Fifth Lumbar Cord

Because pathogenic CD4<sup>+</sup> T cell transfers included both Th1 and Th17 cells (Ogura et al., 2008) (data not shown), we next investigated whether cytokines from these pathogenic CD4<sup>+</sup> T cells contribute to the CD4<sup>+</sup> T cell accumulation in the fifth lumbar cord. For this purpose, we employed IFN $\gamma$ -deficient and IL-17A-deficient mice and immunized them with the MOG peptide plus CFA to obtain pathogenic CD4<sup>+</sup> T cells lacking IFN $\gamma$  or IL-17A. We then transferred these pathogenic CD4<sup>+</sup> T cells separately into wild-type C57BL/6 mice to investigate T cell migration. Of these, only pathogenic CD4<sup>+</sup> T cells from IFN $\gamma$ -deficient mice showed an accumulation in the fifth lumbar cord like that seen in normal pathogenic CD4<sup>+</sup> T cells (Figure 2A), suggesting a role for IL-17A.

We have previously shown that Th17 cells accumulate in joints in a manner dependent on activating the IL-6 amplifier (Murakami et al., 2011), suggesting that the amplifier might be involved in the above accumulation. Pathogenic CD4<sup>+</sup> T cells were intravenously transferred into mutant mice deficient of IL-6 or of either *gp130* or *STAT3* in their type 1 collagen<sup>+</sup> cells and into wild-type C57BL/6 mice. Pathogenic CD4<sup>+</sup> T cell accumulation was significantly suppressed in all mutant hosts (Figure 2B), suggesting that, indeed, IL-6 amplifier activation was involved. We also found the clinical EAE scores in these mutant mice to be significantly suppressed (data not shown) and the IL-6 concentrations in serum to have decreased (Figure 2C). We next identified important type 1 collagen<sup>+</sup> cell populations for pathogenic CD4<sup>+</sup> T cell accumulation in the fifth lumbar cord, because these cell populations include fibroblasts, endothelial cells, epithelial

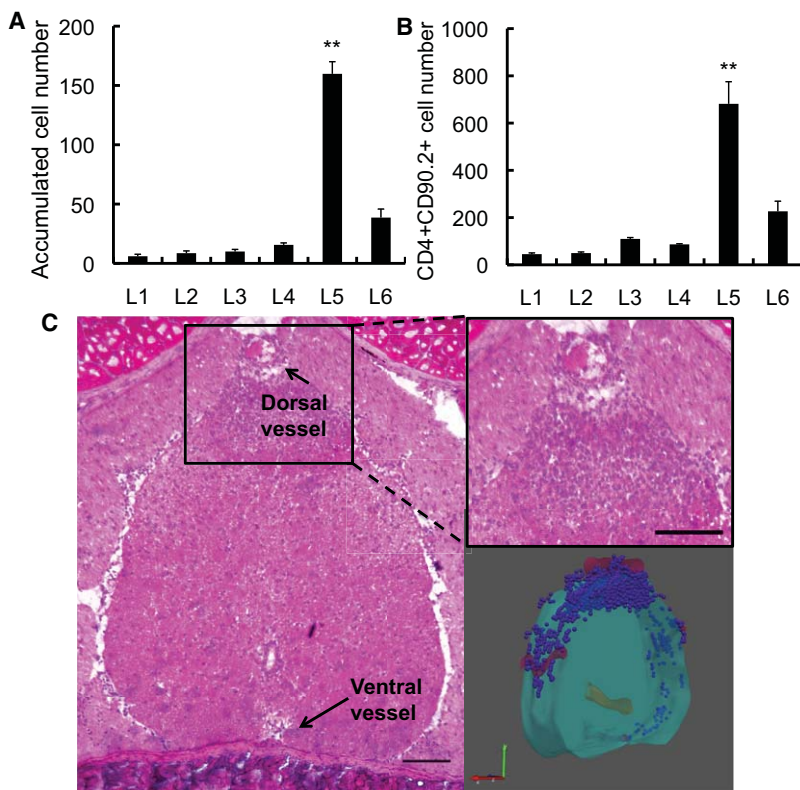


**Figure 1. Pathogenic CD4+ T Cells Transferred to the Blood Mainly Migrate to the CNS from the Fifth Lumbar Cord during the Early Stages of EAE Development**

(A) Pathogenic CD4+ T cell numbers in each spinal cord. Pathogenic CD4+ T cells prepared from wild-type mice transferred into wild-type hosts. The numbers of accumulated pathogenic CD4+ T cells in the six lumbar cords were evaluated by counting mononuclear cells in six different spinal sections (anterior-terminal, middle anterior-center, center, middle center-posterior, and posterior-terminal) and taking the average. Accumulated mononuclear cells in the fifth lumbar cord increased comparing to other cords.

(B) Flow cytometry of mononuclear cells isolated from each spinal lumbar cord. CD4+CD90.2+ cell numbers in the fifth lumbar cord increased comparing to other cords. (C) Pathogenic CD4+ T cells isolated from EAE mice were intravenously transferred into wild-type C57BL/6 mice. Accumulation of pathogenic CD4+ T cells in the choroid plexus and each spinal cord were observed in frozen sections taken 5 days after the transfer. Left: Histological analysis was performed with sections stained with hematoxylin-eosin in the central region of the fifth lumbar cord. Representative data are shown. The scale bar represents 100  $\mu$ m. Top right: Magnification of black rectangle. The scale bar represents 100  $\mu$ m. Bottom right: 3D picture based on ten serial HE sections of the fifth lumbar cord central region. Purple balls indicate nucleuses of pathogenic CD4+ T cell nuclei; red tubes, vessels on the fifth spinal cord.

Error bars represent the mean  $\pm$  SEM. \*\* $p < 0.01$ . See also Figures S1 and S5.

cells, astrocytes, and activated neuron cells. Pathogenic CD4+ T cells were also transferred into mutant mice with Tie2+ endothelial cells deficient of *gp130* and into wild-type C57BL/6 mice. Pathogenic CD4+ T cell accumulation and clinical EAE scores were significantly suppressed in these mutant hosts (Figures S1B and S1C), suggesting the importance of type 1 collagen+ endothelial cells in the accumulation of pathogenic CD4+ T cell in the fifth lumbar cord.

Consistent with these results, STAT3 activation was enhanced in the endothelial cells of dorsal blood vessels in the fifth lumbar cord, but neither in the fourth nor sixth lumbar cords, as determined by STAT3 phosphorylation levels (Figure 2D). These results indicate IL-6 amplifier activation in endothelial cells has a significant role in pathogenic CD4+ T cell accumulation in the fifth lumbar cord during EAE development.

#### CCL20 Expression Contributes to the Accumulation of Pathogenic CD4+ T Cells in the Fifth Lumbar Cord

We next attempted to identify a critical target molecule for STAT3 and NF $\kappa$ B activation in type 1 collagen+ endothelial cells during IL-6 amplifier activation. We considered chemokines like CCL20, because they are synergistically expressed via STAT3 and NF $\kappa$ B in type 1 collagen+ cells, are critical for Th17 cell accumulation in an arthritis model (Murakami et al., 2011), and because pathogenic CD4+ T cells from mice deficient of *CCR6*, a CCL20 receptor, showed minimal accumulation in the fifth lumbar cord (Figure S2A). We found that CCL20 expression in the dorsal blood vessels of the fifth

lumbar cord increased even in the absence of pathogenic CD4+ T cell transfer (Figure 3A), with no such concomitant effect in vessels of the thoracic and cervical cords (Figure S2B). Interestingly, CCL20 expression eventually reached other regions like the anterior lumbar cords after pathogenic CD4+ T cell transfer (Figure S2C, right), suggesting that the blood-brain barrier is compromised broad regions after pathogenic T cell accumulation in the CNS. Furthermore, along with CCL20, chemokines such as CCL2, CCL3, CCL9, CCL21, CCL24, CX3CL1, CXCL1, CXCL2, CXCL9, and CXCL11 increased in the dorsal blood vessels of the fifth lumbar cord compared to the first lumbar cord (Figures 3A and 3B), while anti-CCL20 antibody treatment in vivo significantly suppressed pathogenic CD4+ T cell accumulation and the development of EAE (Figures 3C– 3E).

We next investigated for correlations between CCL20 expression and IL-6 amplifier activation in the fifth lumbar cord. Again, mutant mice deficient of *IL-6* or of either *gp130* or *STAT3* in their type 1 collagen+ cells were employed. CCL20 messenger RNA (mRNA) expressions in the dorsal blood vessels of the fifth lumbar cord was less in all three mutant recipients than in wild-types (Figure 3F). Together with the importance of IL-17A and CCR6 expression in pathogenic CD4+ T cells, these results suggest that CCL20 expression, which is known to be regulated by IL-6 amplifier activation, at least in joints, plays a similar role in pathogenic CD4+ T cell accumulation in the fifth lumbar cord and that this leads to EAE development.

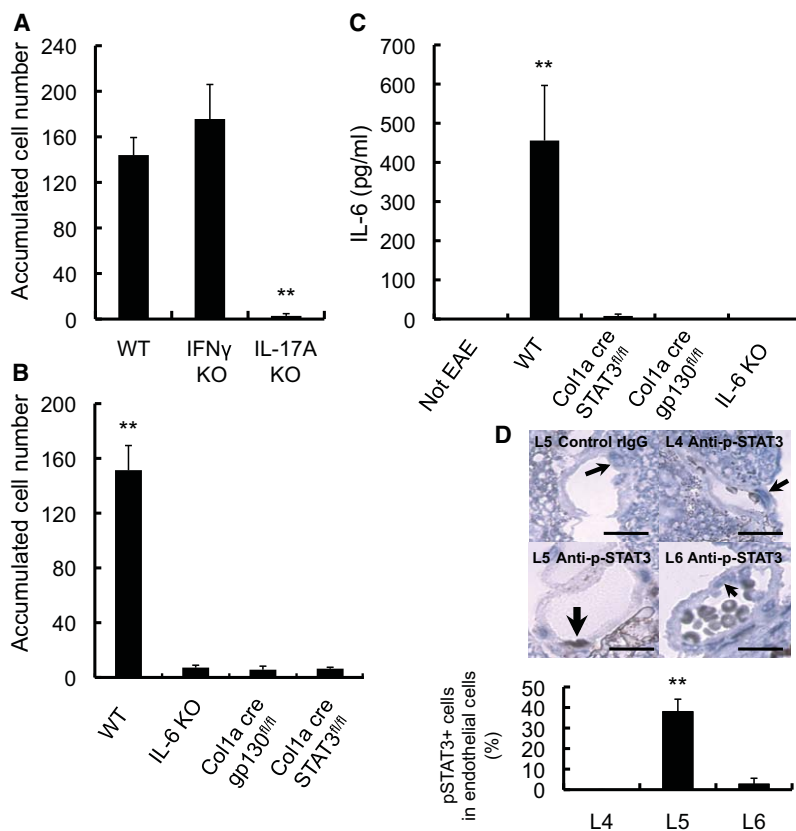


**Figure 2. Activation of IL-6-Mediated Amplification Plays a Role in Pathogenic CD4+ T Cell Accumulation in the Fifth Lumbar Cord**

(A) Pathogenic CD4+ T cells prepared from *IL17A*-deficient, *IFN $\gamma$* -deficient, or wild-type mice were transferred into wild-type hosts. Relative numbers of accumulated pathogenic CD4+ T cells in the fifth lumbar cord. Accumulated mononuclear cells in the fifth lumbar cord decreased after transfer of *IL-17A*-deficient T cells comparing to that of wild-type ones.

(B) Pathogenic CD4+ T cells prepared from wild-type mice were transferred into mutant hosts deficient of *IL-6* or of either *gp130* or *STAT3* in their type 1 collagen+ cells. Relative numbers of accumulated pathogenic CD4+ T cells in the fifth lumbar cord.

(C) Serum IL-6 concentrations in the mutant hosts described in (B). Serum IL-6 decreased in all mutant mice comparing to wild-type ones.

(D) Top: Histological analysis was performed with frozen sections stained with anti-phospho-STAT3 antibody or control rabbit IgG plus secondary antibody. The fourth, fifth, and sixth lumbar cords are shown. Arrows indicate endothelial cell nuclei in the dorsal blood vessels of each lumbar cord. Scale bars represent 50  $\mu$ m. Bottom: Quantification of the histological analysis ( $n = 300$  cells for each lumbar cord). Phospho-STAT3+ endothelial cell numbers increased in the fifth lumbar cords comparing to the fourth and sixth ones.

Error bars represent the mean  $\pm$  SEM, \*\* $p < 0.01$  (A)–(C). Error bars represent the mean  $\pm$  SD (D), \*\* $p < 0.01$ . See also Figure S1.

### Sensory Nerve Activation via Soleus Muscles Is Critical for CCL20 Expression in the Fifth Lumbar Cord and the Ensuing Pathogenic CD4+ T Cell Accumulation

We then considered how the IL-6 amplifier in dorsal blood vessels of the fifth lumbar cord is activated to express CCL20 prior to pathogenic CD4+ T cell transfer. We focused on the activation of soleus muscle-mediated sensory nerves, because their dorsal root ganglia locate near the fifth lumbar (Ohira et al., 2004). We hypothesized that frequent stimulation of the soleus muscles in response to a gravitational stimulus could induce activation of the IL-6 amplifier via their sensory nerves, which in turn would directly or indirectly induce high CCL20 expression in the blood vessels of the fifth lumbar cord. For this, we employed a tail suspension model, which is a widely accepted National Aeronautics and Space Administration ground-based model for studying disuse-atrophy in rodents to eliminate any response by the hind legs to the stimulus (Canu and Garnier, 2009; De-Doncker et al., 2005; Kawano et al., 2007; Nakao et al., 2009). Tail suspensions significantly decreased CCL20 expression in dorsal blood vessels of the fifth lumbar cord (see the left two columns in Figure 4A). Consistent with this, tail suspensions also significantly suppressed pathogenic CD4+ T cell accumulation in the fifth lumbar cord (Figure 4B), while pathogenic CD4+ T cell accumulation and CCL20 expression in cervical cord blood vessels increased, especially in the posterior side (Figure 4B and Figure S3A). Moreover, *c-fos* expression levels decreased in fifth dorsal root ganglia (Figure 4C), but increased in the dorsal root ganglia of the cervical spine after

tail suspension (Figure S3B). Finally, EAE development was significantly inhibited when the tail was suspended (Figure 4D).

In normal mice without pathogenic CD4+ T cell transfer, NF $\kappa$ B activation, which like STAT3 activation is also critical for IL-6 amplifier activation, was enhanced in the blood vessels of the fifth lumbar cord, but not in those of the first lumbar or cervical cords (Figure 4E). Tail-suspended mice, however, responded differently, as NF $\kappa$ B activation was enhanced in vessels of the cervical cord, but not those of the first or fifth lumbar cords (Figure 4E). These data strongly suggest sensory nerve activation by the soleus muscles plays a role in CCL20 expression in the dorsal vessels of the fifth lumbar cord prior to the development of autoimmune diseases that occur from an accumulation of pathogenic CD4+ T cells. To confirm this, we stimulated soleus muscles directly by using an electronic stimulator while mice were suspended from their tails. Electronic stimulations in the soleus muscles increased CCL20 expressions in the dorsal blood vessels in a manner dependent on stimulus duration (see the right four columns in Figure 4A). These stimulations also increased the number of pathogenic CD4+ T cells in the fifth lumbar cord (Figure 4B) and *c-fos* expression in the fifth lumbar dorsal root ganglia (Figure 4C). All these results are consistent with regional neural activations via soleus muscle-mediated sensory nerve activation creating gates for pathogenic CD4+ T cell accumulation into the CNS.

For further validation of our tail suspension model, five additional experiments were done. In the first, electrically stimulating the quadriceps, whose afferent nerves come from the third

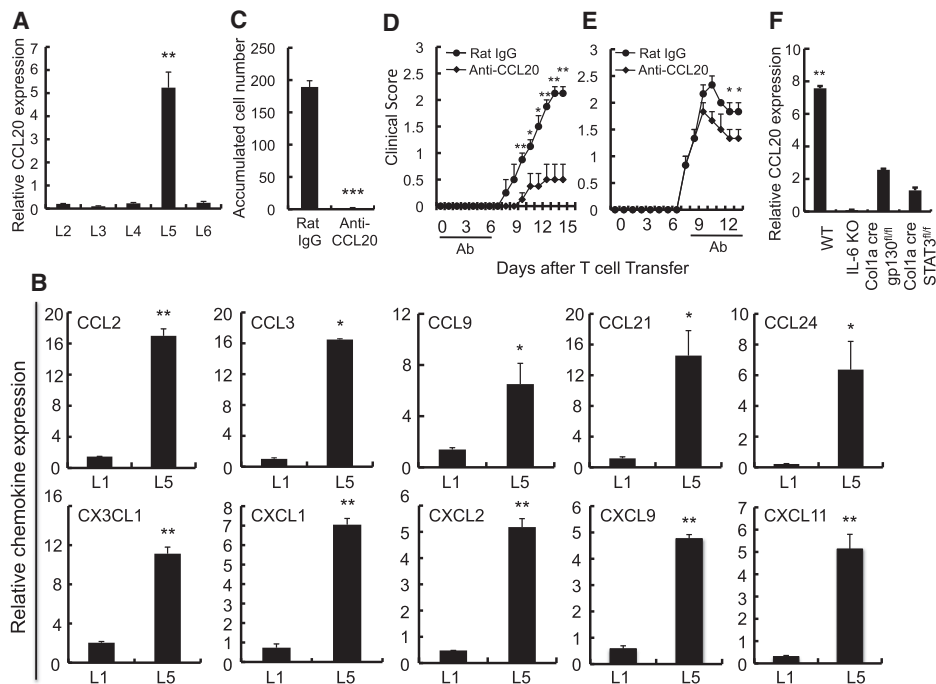


**Figure 3. CCL20 Expression Plays a Role in Pathogenic CD4<sup>+</sup> T Cell Migration in the Fifth Lumbar Cord**

(A) CCL20 mRNA expression in the dorsal blood vessels in each spinal cord was investigated by real time PCR in normal C57BL/6 mice. CCL20 expression in the fifth lumbar cord increased comparing to other cords.

(B) CCL2, CCL3, CCL9, CCL21, CCL24, CX3CL1, CXCL1, CXCL9, and CXCL11 mRNA expression in the dorsal blood vessels of each spinal cord were investigated by real-time PCR in normal C57BL/6 mice.

(C) Pathogenic CD4<sup>+</sup> T cells isolated from EAE mice were intravenously transferred into wild-type C57BL/6 mice in the presence or absence of anti-CCL20 antibody administration (days 0–5 or 8–13 after the pathogenic CD4<sup>+</sup> T cell transfer). Relative accumulation of pathogenic CD4<sup>+</sup> T cells in the fifth lumbar cord were investigated with sections from mice 5 days after the pathogenic T cell transfer.

(D and E) Clinical EAE scores of the mice (n = 10 each) described in (C).

(F) CCL20 mRNA expression in the dorsal blood vessels of the fifth lumbar cord, in wild-type C57BL/6 and mutant mice deficient of *IL-6* or of *gp130* or *STAT3* in their type 1 collagen<sup>+</sup> cells. CCL20 expression in the fifth lumbar cord decreased in all mutant mice comparing to wild-type ones.

Error bars represent the mean  $\pm$  SEM, \*p < 0.05, \*\*p < 0.01, \*\*\*p < 0.005 (A and C–F). Error bars represent the mean  $\pm$  SD, \*p < 0.05, \*\*p < 0.01 (B). See also Figure S2.

lumbar dorsal root ganglia, and the epitrochlearis/triceps brachii, whose afferent nerves come from between the fifth cervical and fifth thoracic dorsal root ganglia, caused CCL20 expression to increase in the third lumbar vessels and between the fifth cervical and fifth thoracic vessels, respectively (Figure S3C). Similarly, these stimulations increased *cfos* expression (Figure S3D). We next employed a deafferentation method where afferent fibers of the fifth lumbar dorsal root ganglia were resected to reduce the soleus muscle response against gravity while only making minimal changes to body balance (Kawano et al., 2007). We found CCL20 expression in the fifth lumbar vessels decreased just like that in the tail suspension model, while CCL20 expression in the first lumbar vessels were unchanged (Figure S3E). Furthermore, *cfos* expression decreased in dorsal root ganglia of the fifth lumbar cords (Figure S3F). We employed tail suspensions plus a casting, as this combination is reported to increase dorsal root ganglion activation (Kawano et al., 2002), finding the increase in CCL20 expression in the fifth lumbar vessels was even greater than tail suspension alone (Figure S3G). Finally, we investigated blood flow speed in blood vessels of the fifth lumbar dorsal region, bottoms of the forefeet, palms, femoral vessels, brain

surface vessels, portal vein, and intestinal microvessels in normal and tail suspended mice. In all cases, speeds were comparable for all investigated regions between the two mouse types except for the fifth lumbar region (Figure S3H). These results demonstrate the viability of our tail suspension model and indicate that regional neural activations create gates for pathogenic CD4<sup>+</sup> T cell entry into the CNS by increasing CCL20 expression.

#### **Soleus Muscle-Mediated Sensory Nerve Activation at Least Partially Enhances CCL20 Expression in the Fifth Lumbar Cord via Sympathetic Neurons**

Finally, we considered how sensory nerve activations from soleus muscles change the state of dorsal vessels of the fifth lumbar cord to cause an accumulation of pathogenic CD4<sup>+</sup> T cells. Continuing the blood flow speed experiments described above, we found electrically stimulating soleus muscles can change fifth lumbar blood flow speed (Figure 5A). Additionally, treatment with the norepinephrine antagonist atenolol significantly suppressed CCL20 mRNA expression, NF $\kappa$ B activation, and pathogenic CD4<sup>+</sup> T cell accumulation around these vessels and abrogated EAE development (Figures 5B–5F). Similar results were obtained

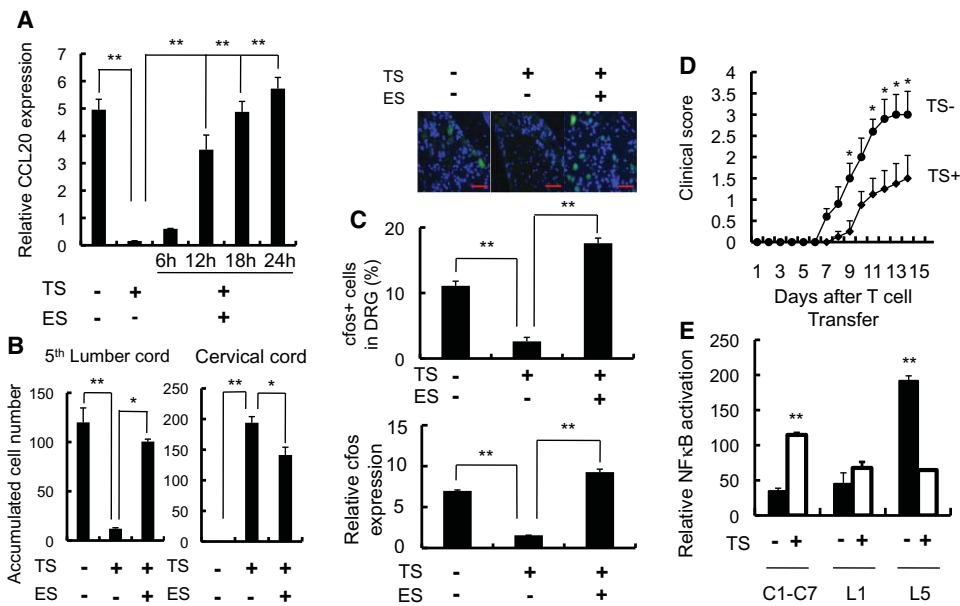


**Figure 4. Sensory Nerve Activation via Soleus Muscle Stimulation Is Critical for CCL20 Expression in the Fifth Lumbar Cord and Pathogenic CD4+ T Cell Accumulation**

(A) CCL20 mRNA expression in dorsal blood vessels of the fifth lumbar cord in wild-type C57BL/6 mice with or without tail suspension (TS) in the presence or absence of soleus muscle electrostimulation (ES).

(B) Accumulation of pathogenic CD4+ T cells in the fifth lumbar cord or spinal cords in the cervical spines of wild-type C57BL/6 mice that received transfusions of pathogenic CD4+ T cells isolated from EAE mice. Mice were grouped as with or without TS and ES. Relative accumulations were measured from sections 5 days after the pathogenic T cell transfer.

(C) Top: Histological analysis with frozen sections stained with anti-cFos antibody (cFos). Representative data from the dorsal root ganglion beside the fifth lumbar cords of the mice described in (B) are shown. Green, cFos molecules; blue, nuclei. Experiments were performed at least three times. Scale bars represent 50  $\mu$ m. Middle: Quantification of histological analysis ( $n = 300$  cells each). Bottom: *c-fos* mRNA expression in the dorsal root ganglia of the fifth lumbar cord. Stimulations lasted 12 hr.

(D) Clinical EAE scores ( $n = 5$  for each group).

(E) NF $\kappa$ B activation monitored by luciferase activity in the dorsal blood vessels of the first lumbar cord (L1), fifth lumbar cord (L5), and spinal cords in the cervical spines (C1–C7) of C57BL/6 mice transduced with a NF $\kappa$ B reporter with or without TS. NF $\kappa$ B activation in the fifth lumbar cord increased comparing to other lumbar cords without tail suspension, while that in the cervical cords increased comparing to other lumbar cords after tail suspension. Dorsal blood vessels were isolated under a stereoscopic microscope.

Error bars represent the mean  $\pm$  SEM, \* $p < 0.05$ , \*\* $p < 0.01$  (A, B, D, and E). Error bars represent the mean  $\pm$  SD, \*\* $p < 0.01$  (C). See also Figure S3.

using another norepinephrine antagonist, prazosin (Figure S4). Furthermore, about 15% of sympathetic nerves in fifth lumbar spine ganglia expressed *c-fos* molecules, while first lumbar spine ganglia did not, which is consistent with CCL20 expression in their dorsal vessels (Figure 5G). Consistent with these *in vivo* results, norepinephrine enhanced IL-6 amplifier activation based on IL-6 or CCL20 expression levels *in vitro* (Figures 5H and 5I). Taken together, these results indicate that sympathetic nerve activation induced by soleus muscles is at least partially involved in the enhanced expression of chemokines like CCL20 in dorsal blood vessels, and that this leads to an accumulation of pathogenic CD4+ T cells in the fifth lumbar cord (Figure 5J). All these results demonstrate that regional neural activations via the soleus muscle-mediated sensory nerve enable pathogenic CD4+ T cell entry into the CNS from adjacent blood vessels.

## DISCUSSION

Although it is known that autoimmune diseases can correlate with neurological states like stress, how neural signals are phys-

ically transformed into an immune response in the CNS is poorly understood. In the current study, we describe how regional neural activations can create gates in specific blood vessels that allow for immune cell entry into the CNS. We employed sensory neural activations of the soleus muscles, finding sympathetic nerve activations here lead to excess CCL20 expression in the fifth lumbar cord in a manner dependent on the activation of the IL-6 amplifier. This in turn leads to the activation of NF $\kappa$ B and STAT3 in type 1 collagen+ endothelial cells. Therefore, neuroimmune interactions induce regional alterations in blood vessels and venules such that immune cells can enter the CNS. When pathogenic helper T cells are in the blood stream, these neuroimmune interactions risk the development of autoimmune disease.

IL-6 amplifier activation has been shown to be critical for the development of autoimmune diseases like EAE and rheumatoid arthritis (Hirano, 2010; Murakami et al., 2011; Ogura et al., 2008). We recently proposed a mechanism that depends on local IL-6-amplifier activation to explain the development of MHC class II-associated diseases as a four-step model for autoimmune diseases. This model shows four local events that must occur

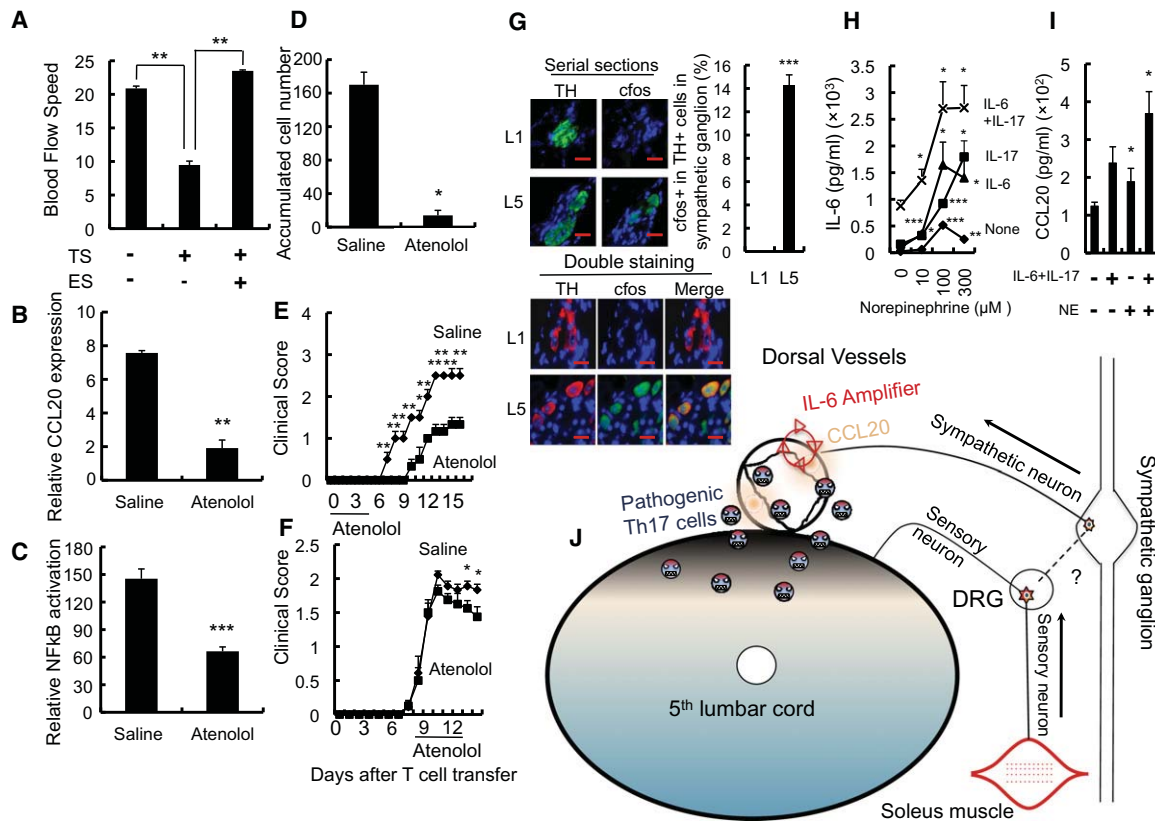


**Figure 5. Soleus Muscle-Mediated Sensory Nerve Activation at Least Partially Enhances IL-6 Amplifier Activation via Sympathetic Neurons**

(A) Blood flow in the dorsal vessel of the fifth lumbar cord in wild-type C57BL/6 with or without tail suspension (TS) in the presence or absence of soleus muscle electrostimulation (ES).  
 (B) CCL20 mRNA expression in vessels from wild-type C57BL/6 mice with or without atenolol treatment.  
 (C) NFκB activation monitored by luciferase activity in vessels from C57BL/6 mice transduced with a NFκB reporter with or without atenolol treatment.  
 (D) Pathogenic CD4+ T cells isolated from EAE mice were intravenously transferred into wild-type C57BL/6 mice. Relative accumulation of pathogenic CD4+ T cells in the fifth lumbar cord of wild-type mice with or without atenolol treatment (days 0–5 or 8–13 after the pathogenic CD4+ T cell transfer).  
 (E and F) Clinical EAE scores (n = 5 for each group).  
 (G) Top left: Histological analysis using serial frozen sections stained with anti-tyrosine hydroxylase antibody (TH) or anti-cFos antibody (cFos). Sympathetic first and fifth lumbar ganglia are shown. Green, TH and cFos, respectively, in the sympathetic ganglion beside the fifth lumbar cord; blue, nuclei. Scale bars represent 50 μm. Representative data are shown. Top right: Histological analysis after double staining with chicken anti-tyrosine hydroxylase antibody (TH, red) or rabbit anti-cFos antibody (cFos, green). Blue, nuclei. Scale bars represent 25 μm. Bottom: Quantification of histological analysis based serial frozen sections (top left) (n = 300 cells for each group).  
 (G–I) IL-6 amplifier activation was enhanced in the presence of norepinephrine. BC1 cells stimulated with human IL-6 plus soluble IL-6 receptor and/or IL-17A for 48 hr in the absence or presence of norepinephrine (G, 10–300 μM; H, 100 μM). Culture supernatants were collected and assessed using an ELISA specific for mouse IL-6 (H) and CCL20 (I). IL-6 and CCL20 concentrations increased in the presence of norepinephrine in each condition.  
 (J) Schematic figure of neural activation-induced pathogenic T cell accumulation in the CNS. Neural activation-mediated IL-6 amplifier enhancement in endothelial cells of dorsal blood vessels in the fifth lumbar cord induces CCL20 followed by the accumulation of pathogenic Th17 cells, a critical event for the development of EAE.

Error bars represent the mean ± SEM, \*p < 0.05, \*\*p < 0.01, \*\*\*p < 0.005 (A–F). Error bars represent the mean ± SD, \*p < 0.05, \*\*p < 0.01, \*\*\*p < 0.005 (G–I). See also Figure S4.

prior to chronic activation of the IL-6 amplifier and subsequent chronic inflammation in the affected tissue: (1) activation of CD4+ T cells regardless of the antigen-specificity, (2) triggering factors for local accumulation of CD4+ T cells, (3) transient activation of the IL-6 amplifier in local tissues by cytokines from the CD4+ T cells, and (4) increased sensitivity to the cytokines in these local tissues (Murakami and Hirano, 2011). Furthermore, it is likely that each step interacts with the others, the degree of which varies with the pathogenesis of the disease. Our current

results lead us to propose that neural activation may contribute to steps 2 or 4.

Sensory neural activation of the soleus muscles activated sympathetic neurons. This was followed by CCL20 expression via IL-6 amplifier activation. That sympathetic nerves are involved is consistent with other reports in which EAE was induced by systemic immunization in the presence or absence of norepinephrine antagonists (Brosnan et al., 1985; Dimitrijević et al., 2007). We suspect increased blood flow speed in the fifth

lumbar cord is a direct or indirect effect of the exercise pressor reflex, which is an example of sensory neuron stimulation that leads to sympathetic neuron activation (Kaufman and Hayes, 2002; Smith et al., 2006). Activation of this reflex changes blood pressure or blood flow via alterations in the blood vessel, particularly those in muscle (Kaufman and Hayes, 2002; Smith et al., 2006). However, it is still an open question on how sensory neurons via the soleus connect to sympathetic neurons and the sympathetic ganglion. We suspect this connection occurs at the dorsal root ganglia of the fifth lumbar cord, since even though sympathetic axons exist in normal dorsal root ganglia they increase in number following a sensory neuron injury (Xie et al., 2010).

Unlike mice, patients suffering from MS do not always display symptoms in their lower body. Instead, MS symptoms are generally isolated in the upper body, particularly the thoracic cord and cerebrum. This difference might be due to different sites for the pathogenic CD4<sup>+</sup> T cell accumulation that follows local inflammation. Because different regional neural activation-mediated CCL20 expression were induced by stimulating several muscles such as the soleus muscles, the quadriceps, and epitrochlearis/triceps brachii (Figure 4A and Figures S3C and S3D), we believe that excess sensory stimulations in other regions like the hands, fingers, and optic nerves, and even less visceral locations like chronic mental stress may affect MS symptoms by promoting excess neural activations and IL-6 amplifier activation in vessels of the thoracic cord and/or cerebrum. Such a theory could also help explain the effects of acupuncture, which involves directly stimulating peripheral nerves to change body homeostasis (Longhurst, 2010). We therefore hypothesize that acupuncture effects may arise by changing the blood vessel status of the target organ.

In the rat transfer models, pathogenic T cells migrate to the spleen prior to entering the CNS (Matsumoto et al., 1988; Panitch, 1980). That we found pathogenic CD4<sup>+</sup> T cells negligibly accumulate in the fifth lumbar cord by day 4 is consistent with this. However, we also found that the fifth lumbar cord shows chemokine expression even in the steady state (Figures 3A and 3B). Such an observation suggests that the transferred pathogenic CD4<sup>+</sup> T cells need not wait until day 4, as they can instead enter the spinal cord using this axis directly. One reason we did not find earlier T cell accumulation may be that the pathogenic CD4<sup>+</sup> T cells express relatively low levels of CCR6 after in vitro culture. That would explain why CCR6 expression levels increased following pathogenic CD4<sup>+</sup> T cell division in the superficial lymph nodes, aortal lymph nodes, mesenteric lymph nodes, and spleens on day 4 after the transfer (Figure S5) and that deficient CCR6 in pathogenic CD4<sup>+</sup> T cells suppressed early T cell entry into the CNS (Figure S2A). Additionally, CCL20 or adrenergic inhibition reduced EAE development, particularly for the first 5 days after pathogenic CD4<sup>+</sup> T cell transfer (Figures 3D and 5E), while anti-CCL20 or an adrenergic receptor inhibitor from day 8 after the pathogenic CD4<sup>+</sup> T cell transfer upon indications of slight tail polarization (Figures 3E and 5F). These results suggest that both blockades have partial therapeutic effects for multiple sclerosis.

It has been observed that the expression of chemokines like CCL20 in the dorsal vessels of the fifth lumbar cord in response

to soleus muscle stimulation can facilitate immunity against pathogenic invasions or latent infectious states in the CNS (McGavern and Kang, 2011; Salinas et al., 2010). Consistent with this, we found the expression of all observed chemokines increased there. This increase could also signal the recruitment of other cell populations, including nonimmune cells as well as other neural precursor cells including microglia ones. Therefore, regional neural activations may maintain homeostasis of the CNS environment by regulating the entry of various cell types from the blood. These phenomena then may suggest the importance of the IL-6 amplifier, a synergistic signal between NFκB and STAT3, for the accumulation of various cell types including pathogenic T cells by creating a gateway to CNS that depends on various sets of chemokine expressions.

To summarize, we describe an entry site at the dorsal blood vessels of the fifth lumbar cord for blood cells including pathogenic CD4<sup>+</sup> T cells into the CNS. Mechanistic experiments demonstrated that CCL20, which we found to be positively regulated by sensory nerve activation via antigravity soleus muscles, plays a role in this accumulation, and that its expression risks the development of autoimmune diseases when pathogenic CD4<sup>+</sup> T cells are present in the blood stream. More importantly, sensory nerve activation enhances CCL20 expression in these dorsal blood vessels via the activation of sympathetic neurons, meaning neural activation can be transformed into an inflammatory signal that leads to autoimmune disease. The location of this neuroinflammatory transformation may prove a valuable therapeutic target for various neuroimmune diseases including autoimmune and inflammatory diseases and is therefore worthy of more study.

## EXPERIMENTAL PROCEDURES

### Mouse Strains

C57BL/6 mice were purchased from Japan SLC. *IL-6*-deficient mice were provided by Dr. M. Kopf (Max Planck Institute of Immunobiology, Germany) and backcrossed with C57BL/6 mice more than ten times. Type I collagen-Cre mice were provided by Dr. G. Karsenty (Baylor College of Medicine, Houston, TX) and crossed with *STAT3*<sup>fllox/fllox</sup> mice (provided by Dr. S. Akira, Osaka University, Japan) (Takeda et al., 1998) and *gp130*<sup>fllox/fllox</sup> mice (Betz et al., 1998). Tie2-Cre mice were provided by Dr. H. Kawamoto (RIKEN Research Center for Allergy and Immunology, Yokohama, Japan). *IL-17A*-deficient (Iwakura and Ishigame, 2006), NFκB reporter (Sadikot and Blackwell, 2008), *CCR6*-deficient (Varona et al., 2001), and *IFNγ*-deficient (Ueda et al., 2006) mice in a C57BL/6 background were also used. All mice were maintained under specific pathogen-free conditions according to the protocols of the Osaka University Medical School. All animal experiments were performed following the guidelines of the Institutional Animal Care and Use Committees of the Graduate School of Frontier Bioscience and Graduate School of Medicine, Osaka University.

### Passive Transfer of Pathogenic CD4<sup>+</sup> T Cells to Induce EAE

EAE induction was performed as described previously (Ogura et al., 2008). In brief, C57BL/6 mice and *IL-17A*-deficient, *IFNγ*-deficient mice were injected with a MOG (35–55) peptide (synthesized by Sigma) in complete Freund's adjuvant (Sigma-Aldrich, Tokyo) at the base of the tail on day 0 followed by intravenous injection of pertussis toxin (Sigma-Aldrich, Tokyo) on days 0, 2, and 7. On day 10, CD4<sup>+</sup> T cells from the resulting mice were sorted with anti-CD4 microbeads (Milteny, Tokyo). The resulting CD4<sup>+</sup> T cell-enriched population ( $4 \times 10^6$  cells) was cocultured with rIL-23 (10 ng/ml; R&D, Minneapolis) in the presence of MOG peptide-pulsed bone marrow-derived dendritic cells ( $5 \times 10^5$ ) for 2 days. Cells ( $1.5 \times 10^7$ ) were then injected intravenously into

wild-type or mutant mice. Clinical scores were measured as described previously (Ogura et al., 2008).

#### Mononuclear Cell Isolation from Spinal Cords

Mononuclear cells from spinal cords were isolated after cardiac perfusion with PBS as described previously (Sawa et al., 2009).

#### Frozen Section Preparations and Histological Analysis

Spines were harvested and fixed in 4% paraformaldehyde for 12 hr and then displaced with 10% sucrose solution for 12 hr, 20% sucrose solution for 12 hr, and finally 30% sucrose solution for 12 hr (total 48 hr). The resulting spines were embedded in SCEM compound (SECTION-LAB, Japan). The cut surface was covered with an adhesive film (Cryofilm type IIC9, SECTION-LAB, Japan) and frozen sections (10  $\mu$ m) were prepared with a microtome (CM3600XP Leica Microsystems, Germany) according to a method described previously (Kawamoto, 2003). The resulting sections were stained with hematoxylin/eosin and analyzed with a BZ-9000 microscope (KEYENCE).

#### Intracellular Cytokine Staining

The number of Th17 cells *in vivo* was determined as previously described (Nishihara et al., 2007). In brief, T cells from spinal cords were stimulated with MOG peptide presented on LPS-stimulated bone marrow-derived dendritic cells in the presence of GolgiPlug (BD Biosciences, Tokyo) for 6 hr. Intracellular IL-17A and IFN- $\gamma$  were labeled with anti-IL-17A and anti-IFN- $\gamma$  antibodies after surface staining, fixation, and permeabilization.

#### Antibodies and Reagents

The following antibodies were used for flow cytometry analysis: APC-conjugated anti-IFN- $\gamma$  (eBioscience, San Diego) and control IgG1 $\kappa$  (eBioscience, San Diego); FITC-conjugated anti-CD8 (eBioscience, San Diego), anti-CD19 (eBioscience, San Diego), anti-B220 (BD Pharmingen, Tokyo), anti-NK1.1 (eBioscience, San Diego), and anti-I-A/I-E (BioLegend, Tokyo); PE-conjugated anti-IL-17A (eBioscience, San Diego), control IgG2a (eBioscience, San Diego), and anti-I-A/I-E (BioLegend, Tokyo); PE-Cy5-conjugated anti-CD4 (BioLegend, Tokyo); PE-Cy7-conjugated anti-CD4 (BioLegend, Tokyo); Pacific Blue-conjugated anti-CD44 (eBioscience, San Diego) and Streptavidin (Invitrogen, Tokyo); and Biotin-conjugated anti-CD90.2 (eBioscience, San Diego). The following antibodies were used for immunohistochemistry: anti-phospho-STAT3 (Tyr705, D3A7) (Cell signaling), anti-tyrosine hydroxylase (Abcam, Tokyo), anti-cFos (Sigma, Tokyo), and control rabbit IgG (DA1E) (Cell Signaling, Tokyo); and Alexa Fluor 488 goat anti-rabbit IgG (H + L) and Alexa 647 goat anti-chicken IgG (Invitrogen, Tokyo). The following antibodies were used for *in vivo* neutralization: purified anti-mouse CCL20 mAb (R&D, Minneapolis). Atenolol and prazosin were purchased from Sigma-Aldrich, Tokyo. The VECTASTAIN Elite ABC Rabbit IgG Kit and the DAB Peroxidase Substrate kit were purchased from Vector Laboratories, Burlingame.

#### ELISA

IL-6 and IL-17A levels in serum or cell cultures supernatant were determined with ELISA kits (BD Pharmingen, Tokyo; eBioscience, San Diego; or R&D, Minneapolis). CCL20 levels in cell cultures supernatant were determined using ELISA kits (R&D, Minneapolis).

#### Flow Cytometry

For cell surface labeling,  $10^6$  cells were incubated with fluorescence-conjugated antibodies for 30 min on ice. The cells were then analyzed with cyan flow cytometers (Beckman Coulter, Tokyo). The collected data were analyzed with Summit software (Beckman Coulter, Tokyo) and/or Flowjo software (Tree Star, Ashland).

#### Laser Microdissection

Approximately 100 frozen sections (15  $\mu$ m) were fixed with acetic acid/ethyl alcohol (1:19) for 15 min followed by PBS washing for 10 min. Tissues around the dorsal blood vessels were collected by a laser microdissection device, DM6000B (Leica, Tokyo), and prepared for total RNA measurements by the

GenElute Mammalian Total RNA kit (Sigma-Aldrich, Tokyo) and DNase I (Sigma-Aldrich, Tokyo).

#### Real-Time PCRs

A GeneAmp 5700 sequence detection system (ABI, Warrington) and SYBER green PCR Master Mix (Sigma-Aldrich, Tokyo) were used to quantify CCL20 mRNA and HPRT mRNA levels. The PCR primer pairs used for real-time PCRs were as follows: mouse HPRT primers, 5'-GATTAGCGATGATGAACCA GGTT-3' and 5'-CCTCCCATCTCCTTCATGACA-3'; mouse CCL20 primers, 5'-ACAGTGTGGGAAGCAAGTCC-3' and 5'-CCGTGAACCTCTTGACCAT-3'; mouse CCL2 primers, 5'- CCGCTGGAGCATCCACGTGT-3' and 5'- TGGGG TCAGCACAGACCTCTCTCT-3'; mouse CXCL1 primers, 5'- CACAGGGGCGC CTATCGCCAA-3' and 5'- CAAGGCAAGCCTCGGACCAT-3'; mouse CXCL2 primers, 5'- ACCCCACTGCGCCAGACAGAA-3' and 5'- AGCAGCCAGGC TCCTCCTTTCC-3'; mouse CX3CL1 primers, 5'-ACGAAATGCGAAATCATG TGC-3' and 5'-CTGTGTCGTCTCCAGGACAA-3'; mouse CCL3 primers, 5'-TG TACCATGACACTGCAAC-3' and 5'-CAACGATGAATTGGCGTGAA-3'; mouse CCL9 primers, 5'-CCCTCTCCTTCTCATTCTTACA-3' and 5'-AGTCT TGAAGCCCATGTGAAA-3'; mouse CCL21 primers, 5'-GGGTCAGGACTGC TGCCTTA-3' and 5'-CGGGATGGGACAGCCTAAA-3'; mouse CCL24 primers, 5'-CCAAGAAGGGCCATAAGATCTG-3' and 5'-GCCCTTTAGAAGGCTGG TT-3'; mouse CXCL9 primers, 5'-TCCTTTTGGGCATCATCTTCC-3' and 5'- TTTGTAGTGGATCGTGCCTCG-3'; mouse CXCL11 primers, 5'-GGCTTCT TATGTTCAAACAGGG-3' and 5'-GCCGTTACTCGGTAATTACA-3'; and mouse *c-fos* primers, 5'-CGGGTTTCAACGCCGACTA-3' and 5'-TTGGCACT AGAGACGGACAGA-3'. The conditions for real-time PCR were 40 cycles at 94°C for 15 s followed by 40 cycles at 60°C for 60 s. The relative mRNA expression levels were normalized to HPRT mRNA levels.

#### Hindlimb Suspension

Hindlimb suspension was performed as described previously (Kawano et al., 2007; Ohira et al., 2002). In brief, strips of sticky tape (about 5 mm wide and 3 cm long) with good cushion were placed longitudinally on the dorsal and ventral sides of the midtail of the hindlimb-unloaded mouse. These strips were further surrounded cross-sectionally by another strip. Strips were adhered loosely so as to keep the blood flow intact. A string was inserted through the gap between the tail and tape and fastened to the roof of the cage at a height that allowed the forelimbs to support the body weight and prevent the hindlimbs from touching any part of the cage. A mouse could reach food and water freely by using its forelimbs. The attachment to the tail was changed each week so as not to inhibit tail growth and blood flow.

#### Electro Stimulations

In some experiments, hindlimb suspended mice were electrostimulated for 12 hr through the soleus muscle with electrical stimulators (Nippon Koden, Tokyo and Unique Medical, Osaka) at 0.1 mA and 1–8 ms random intervals. Electrostimulations were done for 1 day when investigating pathogenic CD4+ T cell migration and two days when measuring CCL20 mRNA expression.

#### Anti-CCL20 Antibody, Atenolol Treatment, and Prazosin Treatment

Anti-CCL20 antibody (200  $\mu$ g/mouse) or atenolol (500  $\mu$ g/mouse) was interperitoneally injected into C57BL/6 mice (6–8 weeks old) for 5 days in which pathogenic CD4+ T cells were transferred. Atenolol (500  $\mu$ g/mouse) or prazosin (500  $\mu$ g/mouse) was injected into wild-type C57BL/6 mice (6–8 weeks old) for 5 days without the pathogenic CD4+ T cell transfer.

#### Luciferase Assay

Blood vessels from the dorsal side of the fifth lumbar cord or first lumbar cord were harvested. Proteins were collected using a Luciferase Reporter Assay kit (Promega, Tokyo) and total protein amount was adjusted. Luciferase activities were measured by a Luciferase detection device (Promega, Tokyo).

#### Blood Flow Analysis

Blood flow volume was measured in blood vessels from the dorsal side of the fifth lumbar cord in C57BL/6 mice (6–8 weeks old) in the presence or absence of tail-suspensions and/or electrostimulations with Omegazone OZ-1 (Omega wave, Tokyo).

### Statistical Analysis

Student's *t* tests (two-tailed) and ANOVA tests were used for the statistical analysis of differences between two groups and that of differences between more than two groups, respectively.

### SUPPLEMENTAL INFORMATION

Supplemental Information includes five figures and can be found with this article online at doi:10.1016/j.cell.2012.01.022.

### ACKNOWLEDGMENTS

We thank Dr. M. Kopf (Max-Planck-Institute of Immunobiology, Germany) for the *IL-6*-deficient mice, Dr. G. Karsenty (Baylor College of Medicine, Houston, TX) for the type I collagen-Cre mice, and Dr. S. Akira (Osaka University, Osaka, Japan) for the *STAT3<sup>fllox/fllox</sup>* mice. We appreciate the excellent technical assistances provided by Dr. J.-J. Jiang, Ms. A. Okuyama, and Ms. N. Kumai, and thank Ms. R. Masuda for her excellent secretarial work. We thank Dr. M. Yagi and Dr. P. Karagiannis (Osaka University) for carefully reading the manuscript. We are grateful to Dr. Fujio Murakami (Osaka University) for important discussions and advice for how to do the neural experiments and thank Dr. M. Miyasaka (Osaka University) for important discussions about blood vessels for lymphocyte migration. We are also grateful to Dr. Y. Nakatsui and Dr. M. Kinoshita (Osaka University) for important discussions about MS patients and thank Dr. Y. Okuyama and Dr. H. Ogura (Osaka University) for important discussions and carefully reading this manuscript. We thank Dr. Y. Oke (Osaka University) for important discussions about the tail suspension experiment. We thank Jihye Lee for her help in preparing the Graphical Abstract. This work was supported by KAKENHI (Y.A., M.H., T.H., and M.M.), the JST-CREST program (T.H. and M.M.), and the Osaka Foundation for the Promotion of Clinical Immunology (M.M.).

Received: June 27, 2011

Revised: September 21, 2011

Accepted: January 15, 2012

Published: February 2, 2012

### REFERENCES

- Betz, U.A., Bloch, W., van den Broek, M., Yoshida, K., Taga, T., Kishimoto, T., Addicks, K., Rajewsky, K., and Müller, W. (1998). Postnatally induced inactivation of gp130 in mice results in neurological, cardiac, hematopoietic, immunological, hepatic, and pulmonary defects. *J. Exp. Med.* **188**, 1955–1965.
- Brosnan, C.F., Goldmuntz, E.A., Cammer, W., Factor, S.M., Bloom, B.R., and Norton, W.T. (1985). Prazosin, an alpha 1-adrenergic receptor antagonist, suppresses experimental autoimmune encephalomyelitis in the Lewis rat. *Proc. Natl. Acad. Sci. USA* **82**, 5915–5919.
- Canu, M.H., and Garnier, C. (2009). A 3D analysis of fore- and hindlimb motion during overground and ladder walking: comparison of control and unloaded rats. *Exp. Neurol.* **218**, 98–108.
- De-Doncker, L., Kasri, M., Picquet, F., and Falempin, M. (2005). Physiologically adaptive changes of the L5 afferent neurogram and of the rat soleus EMG activity during 14 days of hindlimb unloading and recovery. *J. Exp. Biol.* **208**, 4585–4592.
- Dimitrijević, M., Rauski, A., Radojević, K., Kosec, D., Stanojević, S., Pilipović, I., and Leposavić, G. (2007). Beta-adrenoceptor blockade ameliorates the clinical course of experimental allergic encephalomyelitis and diminishes its aggravation in adrenalectomized rats. *Eur. J. Pharmacol.* **577**, 170–182.
- Felten, D.L. (2000). Neural influence on immune responses: underlying suppositions and basic principles of neural-immune signaling. *Prog. Brain Res.* **122**, 381–389.
- Galea, I., Bechmann, I., and Perry, V.H. (2007). What is immune privilege (not)? *Trends Immunol.* **28**, 12–18.
- Hirano, T. (2010). Interleukin 6 in autoimmune and inflammatory diseases: a personal memoir. *Proc. Jpn. Acad., Ser. B, Phys. Biol. Sci.* **86**, 717–730.
- Iwakura, Y., and Ishigame, H. (2006). The IL-23/IL-17 axis in inflammation. *J. Clin. Invest.* **116**, 1218–1222.
- Kaufman, M.P., and Hayes, S.G. (2002). The exercise pressor reflex. *Clin. Auton. Res.* **12**, 429–439.
- Kawamoto, T. (2003). Use of a new adhesive film for the preparation of multi-purpose fresh-frozen sections from hard tissues, whole-animals, insects and plants. *Arch. Histol. Cytol.* **66**, 123–143.
- Kawano, F., Nomura, T., Ishihara, A., Nonaka, I., and Ohira, Y. (2002). Afferent input-associated reduction of muscle activity in microgravity environment. *Neuroscience* **114**, 1133–1138.
- Kawano, F., Matsuoka, Y., Oke, Y., Higo, Y., Terada, M., Wang, X.D., Nakai, N., Fukuda, H., Imajoh-Ohmi, S., and Ohira, Y. (2007). Role(s) of nucleoli and phosphorylation of ribosomal protein S6 and/or HSP27 in the regulation of muscle mass. *Am. J. Physiol. Cell Physiol.* **293**, C35–C44.
- Longhurst, J.C. (2010). Defining meridians: a modern basis of understanding. *J. Acupunct. Meridian Stud.* **3**, 67–74.
- Matsumoto, Y., Kawai, K., and Fujiwara, M. (1988). Hemorrhagic autoimmune encephalomyelitis induced by adoptive transfer of activated semiallogeneic spleen cells into irradiated rats. *Am. J. Pathol.* **133**, 306–315.
- McGavern, D.B., and Kang, S.S. (2011). Illuminating viral infections in the nervous system. *Nat. Rev. Immunol.* **11**, 318–329.
- Murakami, M., and Hirano, T. (2011). A four-step model for the IL-6 amplifier, a regulator of chronic inflammations in tissue-specific MHC class II-associated autoimmune diseases. *Front Immunol.* **2**. Published online June 16, 2011. 10.3389/fimmu.2011.00022.
- Murakami, M., Okuyama, Y., Ogura, H., Asano, S., Arima, Y., Tsuruoka, M., Harada, M., Kanamoto, M., Sawa, Y., Iwakura, Y., et al. (2011). Local micro-bleeding facilitates IL-6- and IL-17-dependent arthritis in the absence of tissue antigen recognition by activated T cells. *J. Exp. Med.* **208**, 103–114.
- Nakao, R., Hirasaka, K., Goto, J., Ishidoh, K., Yamada, C., Ohno, A., Okumura, Y., Nonaka, I., Yasutomo, K., Baldwin, K.M., et al. (2009). Ubiquitin ligase Cbl-b is a negative regulator for insulin-like growth factor 1 signaling during muscle atrophy caused by unloading. *Mol. Cell. Biol.* **29**, 4798–4811.
- Nance, D.M., and Sanders, V.M. (2007). Autonomic innervation and regulation of the immune system (1987-2007). *Brain Behav. Immun.* **21**, 736–745.
- Nishihara, M., Ogura, H., Ueda, N., Tsuruoka, M., Kitabayashi, C., Tsuji, F., Aono, H., Ishihara, K., Huseby, E., Betz, U.A., et al. (2007). IL-6-gp130-STAT3 in T cells directs the development of IL-17+ Th with a minimum effect on that of Treg in the steady state. *Int. Immunol.* **19**, 695–702.
- Ogura, H., Murakami, M., Okuyama, Y., Tsuruoka, M., Kitabayashi, C., Kanamoto, M., Nishihara, M., Iwakura, Y., and Hirano, T. (2008). Interleukin-17 promotes autoimmunity by triggering a positive-feedback loop via interleukin-6 induction. *Immunity* **29**, 628–636.
- Ohira, M., Hanada, H., Kawano, F., Ishihara, A., Nonaka, I., and Ohira, Y. (2002). Regulation of the properties of rat hind limb muscles following gravitational unloading. *Jpn. J. Physiol.* **52**, 235–245.
- Ohira, Y., Kawano, F., Stevens, J.L., Wang, X.D., and Ishihara, A. (2004). Load-dependent regulation of neuromuscular system. *J. Gravit. Physiol.* **17**, 127–128.
- Panitch, H.S. (1980). Adoptive transfer of experimental allergic encephalomyelitis with activated spleen cells: comparison of in vitro activation by concanavalin A and myelin basic protein. *Cell. Immunol.* **56**, 163–171.
- Ransohoff, R.M. (2009). Chemokines and chemokine receptors: standing at the crossroads of immunobiology and neurobiology. *Immunity* **31**, 711–721.
- Reboldi, A., Coisne, C., Baumjohann, D., Benvenuto, F., Bottinelli, D., Lira, S., Uccelli, A., Lanzavecchia, A., Engelhardt, B., and Sallusto, F. (2009). C-C chemokine receptor 6-regulated entry of TH-17 cells into the CNS through the choroid plexus is required for the initiation of EAE. *Nat. Immunol.* **10**, 514–523.

- Sadikot, R.T., and Blackwell, T.S. (2008). Bioluminescence: imaging modality for in vitro and in vivo gene expression. *Methods Mol. Biol.* *477*, 383–394.
- Salinas, S., Schiavo, G., and Kremer, E.J. (2010). A hitchhiker's guide to the nervous system: the complex journey of viruses and toxins. *Nat. Rev. Microbiol.* *8*, 645–655.
- Sawa, Y., Arima, Y., Ogura, H., Kitabayashi, C., Jiang, J.J., Fukushima, T., Kamimura, D., Hirano, T., and Murakami, M. (2009). Hepatic interleukin-7 expression regulates T cell responses. *Immunity* *30*, 447–457.
- Smith, S.A., Mitchell, J.H., and Garry, M.G. (2006). The mammalian exercise pressor reflex in health and disease. *Exp Physiol.* *91*, 89–102.
- Sternberg, E.M. (2006). Neural regulation of innate immunity: a coordinated nonspecific host response to pathogens. *Nat. Rev. Immunol.* *6*, 318–328.
- Takeda, K., Kaisho, T., Yoshida, N., Takeda, J., Kishimoto, T., and Akira, S. (1998). Stat3 activation is responsible for IL-6-dependent T cell proliferation through preventing apoptosis: generation and characterization of T cell-specific Stat3-deficient mice. *J. Immunol.* *161*, 4652–4660.
- Thayer, J.F., and Sternberg, E.M. (2010). Neural aspects of immunomodulation: focus on the vagus nerve. *Brain Behav. Immun.* *24*, 1223–1228.
- Tracey, K.J. (2007). Physiology and immunology of the cholinergic antiinflammatory pathway. *J. Clin. Invest.* *117*, 289–296.
- Ueda, N., Kuki, H., Kamimura, D., Sawa, S., Seino, K., Tashiro, T., Fushuku, K., Taniguchi, M., Hirano, T., and Murakami, M. (2006). CD1d-restricted NKT cell activation enhanced homeostatic proliferation of CD8+ T cells in a manner dependent on IL-4. *Int. Immunol.* *18*, 1397–1404.
- Varona, R., Villares, R., Carramolino, L., Goya, I., Zaballos, A., Gutiérrez, J., Torres, M., Martínez-A, C., and Márquez, G. (2001). CCR6-deficient mice have impaired leukocyte homeostasis and altered contact hypersensitivity and delayed-type hypersensitivity responses. *J. Clin. Invest.* *107*, R37–R45.
- Watkins, L.R., and Maier, S.F. (1999). Implications of immune-to-brain communication for sickness and pain. *Proc. Natl. Acad. Sci. USA* *96*, 7710–7713.
- Wilson, E.H., Weninger, W., and Hunter, C.A. (2010). Trafficking of immune cells in the central nervous system. *J. Clin. Invest.* *120*, 1368–1379.
- Xie, W., Strong, J.A., and Zhang, J.M. (2010). Increased excitability and spontaneous activity of rat sensory neurons following in vitro stimulation of sympathetic fiber sprouts in the isolated dorsal root ganglion. *Pain* *151*, 447–459.